

BBA 77252

“ACTION POTENTIALS” IN *NEUROSPORA CRASSA*, A MYCELIAL FUNGUS

CLIFFORD L. SLAYMAN, W. SCOTT LONG and DIETRICH GRADMANN*

Department of Physiology, Yale School of Medicine, 333 Cedar Street, New Haven, Conn. 06510 (U.S.A.)

(Received October 16th, 1975)

SUMMARY

Occasional spontaneous “action potentials” are found in mature hyphae of the fungus *Neurospora crassa*. They can arise either from low-level sinusoidal oscillations of the membrane potential or from a linear slow depolarization which accelerates into a rapid upstroke at a voltage 5–20 mV depolarized from the normal resting potential (near -180 mV). The “action potentials” are long-lasting, 1–2 min and at the peak reach a membrane potential near -40 mV. A 2- to 8-fold increase of membrane conductance accompanies the main depolarization, but a slight decrease of membrane conductance occurs during the slow depolarization. Two plausible mechanisms for the phenomenon are (a) periodic increases of membrane permeability to inorganic ions, particularly H^+ or Cl^- and (b) periodic decreases in activity of the major electrogenic pump (H^+) of the *Neurospora* membrane, coupled with a non-linear (inverse sigmoid) current-voltage relationship.

Identification of action potential-like disturbances in fungi means that such behavior has now been found in all major biologic taxa which have been probed with suitable electrodes. As yet there is no obvious function for the events in fungi.

INTRODUCTION

The number of biological systems (in addition to the classical excitable tissues of nerve, muscle, and the giant algae) that are now known to display reversible, all-or-none changes in membrane permeability, giving rise to action potentials, is sufficiently large to raise the question of whether essentially all biological membranes may be inherently capable of producing action potentials, given appropriate environmental conditions.

Some of the more interesting non-classical preparations which show action potential-like behavior are (a) frog skin, which reacts to large polarizing currents (0.5 – 1 mA/cm², driving the skin inner surface negative) by producing a transient 5-fold decrease of membrane conductance [1], (b) ciliated protozoa, especially *Paramecium*, whose action potential reflects a large Ca^{2+} flux that triggers ciliary reversal [2],

* Present address: Institut für Biologie I, Universität Tübingen, 7400 Tübingen, West Germany.

(c) motor tissues in plants having rapid leaf movements, such as *Mimosa* and *Biophytum* [3, 4], or the carnivorous plants Venus fly trap (*Dionaea*) [5], and sundew (*Drosera*) [6] and (d) vascular bundles of certain other plants, such as pumpkin (*Curcubita*) [7], sunflower (*Helianthus*) [8] and peas (*Pisum*) [9], where any motor function for action potentials is obscure.

The present paper describes spontaneous voltage oscillations resembling action potentials in a fungus, the ascomycete *Neurospora crassa*. This action potential-like behavior is sluggish, lasting up to 1 min or longer, is associated with a large increase of membrane conductance, and can be more than 175 mV in amplitude. Thus far no function has been identified for either the voltage changes or the associated conductance changes.

MATERIALS AND METHODS

Strains of Neurospora. Three strains of *N. crassa* were used in the present experiments: the wild type, RL21a; the slow-growing strain NSX *fa* (*poky f*), obtained from Dr. D. J. L. Luck, of The Rockefeller University; and the pleiotropic transport mutant, UM300a, given to us by Dr. Roland Davis, of the University of California, Irvine.

Handling the Cells. Except as otherwise noted, all cultures were prepared from a small inoculum grown on the surface of scratched cellophane, which was supported by 2.5 % agar in Vogel's minimal medium [10] plus 2 % sucrose. Plates were incubated 20–40 h at 25 °C, and segments of the colony cut near the growing margin were then removed on the cellophane, washed and transferred to the electrical recording chamber on the stage of a compound microscope.

The recording chamber, described previously [11], consisted of a shallow Lucite well with a coverslip top, and with open sides through which entered the microelectrodes, the reference electrodes and the fluid perfusion ports. 1–3 microelectrodes were inserted into each hypha, with the aid of Huxley micromanipulators [12], and the mechanical setup was shock-mounted on a Lansing vibration isolation system (model 71.402; Lansing Research Corp, Ithaca, N.Y.).

Solutions. Because the observations reported here have been culled from experiments carried out for quite separate purposes, many different recording solutions have been used. The compositions of these are listed in Table I.

Recording apparatus. The microelectrodes used were conventional glass micropipettes, with tip diameters less than 1 μm , filled (vacuum boiling) with 3 M KCl, and having resistance of about 25 M Ω when measured in the usual extracellular solutions. These were connected, via stable Ag-AgCl half cells, to solid-state electrometer amplifiers with input impedances greater than $10^{10} \Omega$, and a leakage current of approx. $5 \cdot 10^{-12}$ A. For resistance measurements, current was passed through an independent microelectrode, connected to an operational amplifier (configured as an adder, and driven by Tektronix 161 pulse generators) through a $10^{10} \Omega$ resistor. Signals from all amplifiers were monitored both on an oscilloscope and on a chart recorder.

Computations and plots. All records of membrane potential are shown with the cell interior (which is electrically negative to the bath) plotted downward, according to the standard electrophysiological convention. Depolarizing disturbances,

TABLE I

COMPOSITIONS OF SOLUTIONS USED IN EXPERIMENTS ON OSCILLATIONS AND "ACTION POTENTIALS"

Label	Concentration (mM)					
	A	B	C	D	E	F
Ion						
K ⁺	10	25	0.1	37	10.7	25
Na ⁺	—	—	25	25	7.3	—
NH ₄ ⁺	1	—	—	—	7.3	—
H ⁺ (pH)	5.8	5.8	5.8	~ 5.8	5.8	5.8
Mg ²⁺	0.5	—	—	—	0.2	—
Ca ²⁺	1	1	1	—	2.5	1
Cl ⁻	3	2	2.1	62	5.0	2
NO ₃ ⁻	1	—	—	—	7.3	—
SO ₄ ²⁻	—	—	—	—	0.2	—
Phosphate	9.1	—	—	—	10.7	23.1
3,3-dimethylglutaric acid	—	20	20	—	—	—
Citrate	—	—	—	—	2.4	—
Sugar						
Glucose	56	56	56	—	56	5
Sucrose	—	—	—	29	—	—
Used in						
Fig.	2, 4, 5, 6	1C, 3	1B	—	1A	1D
Experiment	4	3	—	1	—	2

therefore, are always upward movements of the traces. Stated values of membrane potential have all been corrected (0–10 mV) for the microelectrode tip potential, according to a method described previously [13]. Average values of membrane parameters are stated as mean \pm 1 S.E.M.

RESULTS

Types of voltage oscillations in Neurospora

Several different types of oscillatory changes have been observed in the membrane potential of *Neurospora*. Four of these are illustrated in Fig. 1. The simplest type (Fig. 1A) is a spontaneous, quasi-sinusoidal fluctuation of 10–20 mV amplitude, which persists for varying intervals of time, from 10–15 min to 1 h or more, and which has a constant period of 3–4 min. These oscillations can appear without clear relation to experimental manipulations, but often arise a short time after recovery from an interval of respiratory blockade. Another type of oscillation resembles the first in most respects, but has a distinctly shorter period, 20–30 s (Fig. 1B). It is best observed in the pleiotropic transport mutant UM300, but has also been found in wild-type *Neurospora*.

Oscillations can be elicited at will by respiratory blockade, provided the blockade is incomplete. This situation arises with wild-type *Neurospora*, for example, following a step increase in cyanide concentration applied to cells previously adapted to low levels (or intermittent pulses) of cyanide. During adaptation, a cyanide-insensitive oxidase is synthesized [14], which serves as an auxiliary pathway for ATP

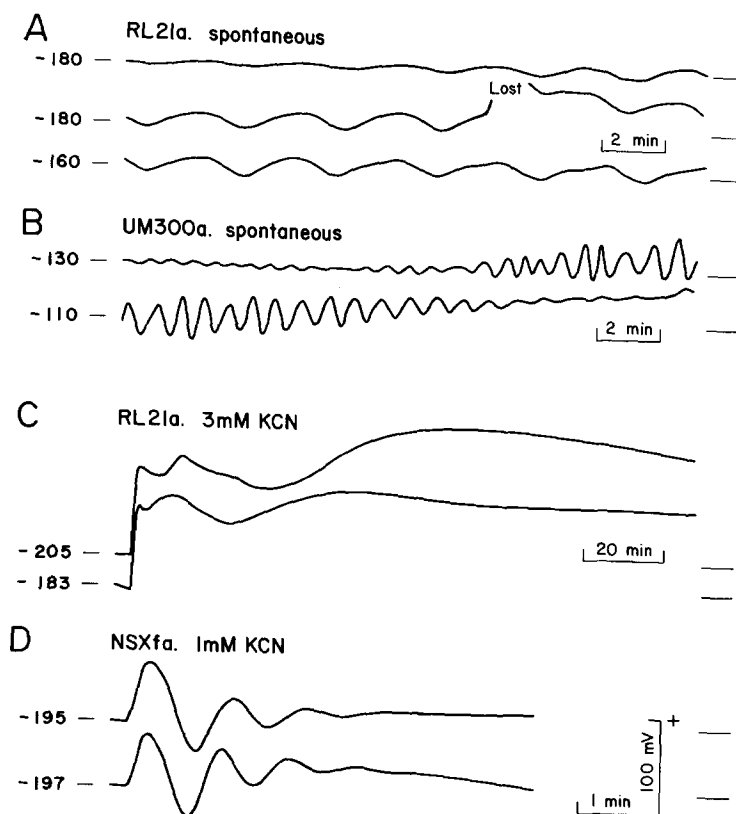


Fig. 1. Four different types of oscillatory behavior of membrane potential in *Neurospora*. (A and B) Spontaneous, low-level sinusoids, of period 3 min and 0.5 min. Successive records in A and in B are continuous. (C) Cyanide-induced oscillations of progressively lengthening period in wild-type hyphae. Note compressed time scale for these two records. (D) Damped sinusoidal oscillations induced by cyanide in the respiratory mutant *poky f*. Cyanide was injected immediately before the sharp upward deflections in the records of C and D. Hyphae punctured for A, C and D were from standard cellophane-agar cultures. Cells for B were from liquid shaking cultures grown under conditions of K^+ limitation, a maneuver which, in the mutant UM300, swells the very small cells characteristic of shaking liquid cultures to a size large enough for microelectrodes. Solutions are listed in Table I. The same voltage scale (bottom right) applies to all records.

synthesis. The sudden step of cyanide then produces oscillations as shown in Fig. 1C. The initial depolarization, also seen with unadapted hyphae, terminates in continuous fluctuations having a variable amplitude of 20–60 mV, an increasing period length (initially 1–2 min) and a duration of 2 h or more. More stereotyped oscillations are obtained in the respiratory mutant *poky f* in response to cyanide treatment. This mutant possesses a large amount of the cyanide-insensitive oxidase (as well as part of the cytochrome pathway) under normal conditions [14], and responds to cyanide as in Fig. 1D. The damped oscillations commence with a peak-to-peak amplitude of 50–100 mV, have periods of 0.5–2 min, persist for 2–4 cycles and usually terminate at a membrane potential 20–30 mV depolarized with respect to the control level [15].

Of the four types of voltage oscillation illustrated in Fig. 1, only the cyanide-induced oscillations in *poky f* are accompanied by measurable oscillations of membrane conductance. (The practical limit of resolution in conductance measurements, by graphic analysis of current- and voltage-pulse data, is about 5 %, and does not preclude the existence of low-level conductance changes for the other cases.) The conductance oscillations in *poky f* occur roughly in phase with the voltage oscillations (conductance decrease synchronized with depolarization), but detailed quantitative analysis has shown the conductance changes to be most simply explained as a consequence, rather than a cause, of the voltage changes. The magnitude of conductance change (± 30 %, for the maximal voltage swings) is that which would be expected from the non-linearity of the normal current-voltage curve in *poky f Neurospora* [15].

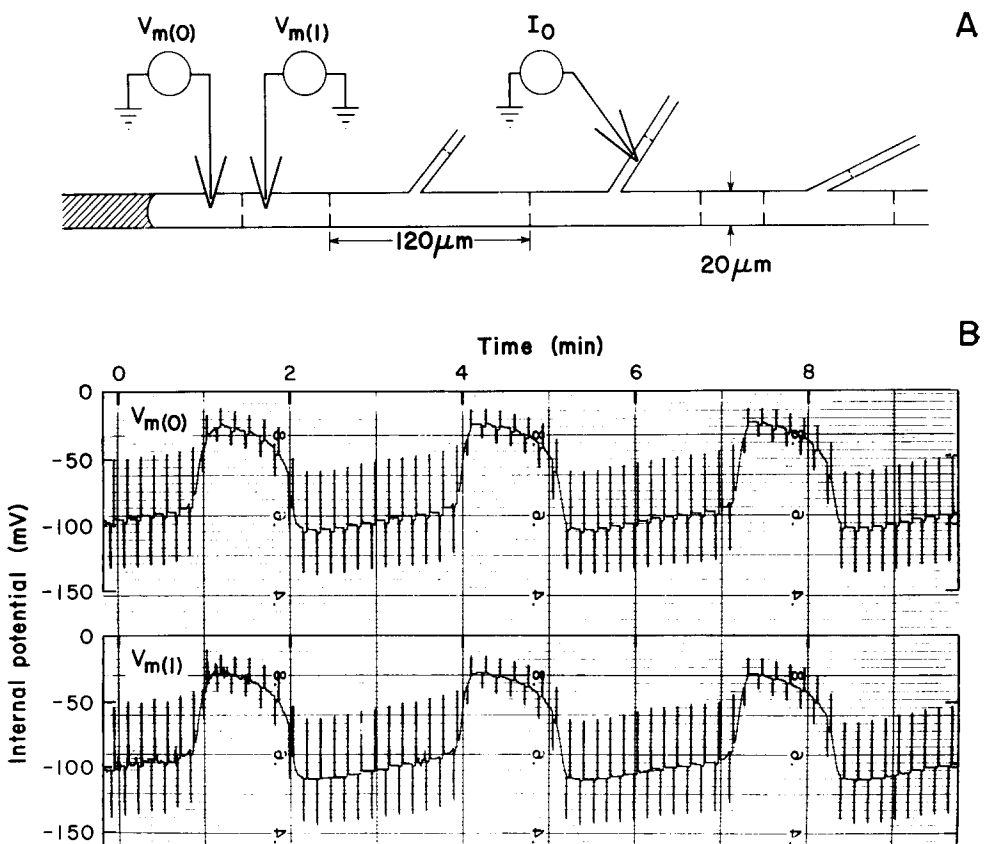


Fig. 2. Train of "action potentials" in *Neurospora*. (A) Scale diagram of the arrangement of micro-electrodes. *Neurospora* hyphae are divided into segments 50–200 μm long by perforate crosswalls, which provide a lumped longitudinal resistance. Shaded area at the left designates a dead segment, which was electrically isolated from the rest of the hyphae by a sealed crosswall. (B) Three "action potentials" from a series of 12, with superimposed current pulses. Current delivered at I_0 : 2.8 nA; 0.5 s–1.5 s off, 0.5 s +; 10-s cycle. Records obtained without the added current pulses are superimposable on these, so the brief shocks had no measurable effect on the time-course of the "action potential". Average properties of all the "action potentials" are listed in Table II.

Description of the action potential-like behavior

A fifth type of oscillatory change in the membrane potential of *Neurospora* differs from those described above in being clearly non-sinusoidal in time course, and in being accompanied by a 2- to 8-fold change of membrane conductance (conductance increase synchronized with depolarization). In basic shape, it resembles the long-duration action potentials seen, for example, in mammalian cardiac fibers [16–18], fluoride-perfused squid axons [19] and *Drosera* tentacles [6]. Its general properties are illustrated in Fig. 2B, which shows two simultaneous records taken from the same hypha during a spontaneous train of 12 “action potentials”. (The superimposed pulses, whose amplitude reflects the membrane resistance, will be discussed in detail below.) Starting from a resting membrane potential of -109 mV (of small magnitude for *Neurospora*), the membrane depolarized slowly and approximately linearly (0.11 mV/s) for 100 s, until the potential reached -94 to -90 mV, at which level depolarization accelerated to 9 mV/s. Depolarization terminated at about -30 mV to form a plateau with slow repolarization (0.6 mV/s); this lasted for approx. 25 s, and merged into a rapid phase of repolarization (again, 9 mV/s). Such action potential-like behavior has been observed in four experiments, with a single event in each of two experiments, a pair of “action potentials” about 6 min apart in a third experiment, and a rhythmic train of 12 in the fourth experiment. Various parameters of this action potential-like behavior are listed in Table II.

In the cases shown in Fig. 2, and for the single event seen in Experiment 2, the rapid upstroke itself appeared to be triggered by slow linear depolarization, but in the other two experiments it arose during normal sinusoidal oscillations in membrane potential, of the types shown in Figs. 1A and 1D. Two such potentials, from

TABLE II

MEASURED PARAMETERS OF “ACTION POTENTIALS” IN *NEUROSPORA*

Three “action potentials” from Experiment 4 are reproduced in Fig. 2; those from Experiment 3 are shown in Fig. 3. “Thresholds” were estimated as the point of intersection of the slow depolarization with the upstroke of the “action potential” (See Fig. 2).

Experiment	1	2	3	4
Number of “action potentials”	1	1	2	12
Membrane potential (mV)				
Resting	-180	-165	-183 ± 3	-111 ± 2
“Threshold”	-172	-143	-180 ± 2	-94 ± 2
Peak of “action potential”	-42	-38	-53 ± 1	-32 ± 2
Middle of plateau	—	-55	-82 ± 9	-37 ± 1
Overshoot, to	—	—	-229 ± 17	—
Maximum ΔV	138	127	176 ± 16	79 ± 1
Rate of polarization (mV/s)				
Slow depolarization	oscillation	0.6	oscillation	0.11 ± 0.02
Maximum rise of “action potential”	2.4	17	6.8 ± 1.0	9.1 ± 0.6
Decay of plateau	—	2.4	3.3 ± 1.7	0.58 ± 0.08
Maximum repolarization	-1.6	-20	-38 ± 13	-8.6 ± 0.9
Time (s)				
Duration slow depolarization	oscillation	20	oscillation	100 ± 2
“Threshold” to peak	117	21	29 ± 1	29 ± 2
Duration of plateau	—	8.2	10 ± 1	24 ± 2
Whole “action potential”	234	40	58 ± 9	84 ± 2

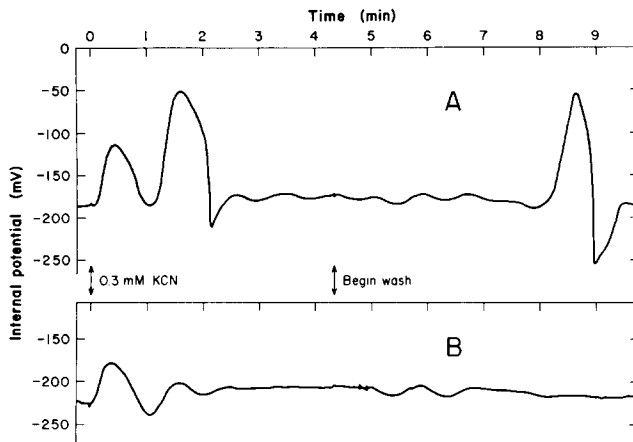


Fig. 3. "Action potentials" arising from cyanide oscillations. Strain NSX *fa* (*poky f*); Experiment 3 in Table II. A and B are simultaneous records from two independent hyphae. Cyanide-induced oscillations are very similar in both hyphae. Action potentials appear in only one.

Experiment 3, are reproduced in Fig. 3. The records in that figure were made during treatment of the *poky f* strain with 0.3 mM KCN. Sinusoidal oscillations followed both cyanide addition (0 time) and cyanide washout (4.3 min) in the two separate hyphae being studied (upper and lower traces). As was generally found for these cyanide-induced oscillations [15], separate hyphae (electrically independent) in a single culture showed oscillations of closely similar amplitude and frequency, presumably reflecting the common metabolic state produced by cyanide inhibition. While the "action potentials" clearly arose during the depolarizing phase of the cyanide-induced (or washout-induced) oscillations, they developed in only one of the two impaled hyphae. This presumably means either that this behavior is not directly caused by a metabolic event, or that the causal event is different from that which produces the typical induced oscillations.

Conductance changes

In two experiments (Experiments 2 and 4) action potential-like behavior was observed during multiple-electrode recordings from single hyphae, and it was possible to inject current through one electrode for the purpose of measuring the membrane conductance. The arrangement of electrodes in Experiment 4 is shown in Fig. 2A. The recording electrodes ($V_{m(0)}$ and $V_{m(1)}$) were placed 32 μm apart, in adjacent "cells", which were blocked at one end by a dead, sealed segment of hypha. A third electrode, used to pass current, was situated 230 μm away (in a small branch hypha, but close to the main hypha).

In *Neurospora*, the longitudinal resistance of the hyphal interior is normally dominated by the crosswall (r_p), rather than by the cytoplasm (r_i), so the membrane current in the 0th cell (end), flowing in response to a finite injected current, is given by $(\Delta V_{m(1)} - \Delta V_{m(0)})/r_p$. Though in this particular experiment we had no independent measure of r_p , it is generally stable near $2\text{M}\Omega$ (Gradmann, D., Slayman, C. L., and Hansen, U. P., manuscript in preparation), provided that the hyphae are not subjected to repeated mechanical damage. The dimensions of the end cell in Fig. 2A were length = 58 μm , diameter = 20 μm , so that $(\Delta V_{m(1)} - \Delta V_{m(0)})$ can be con-

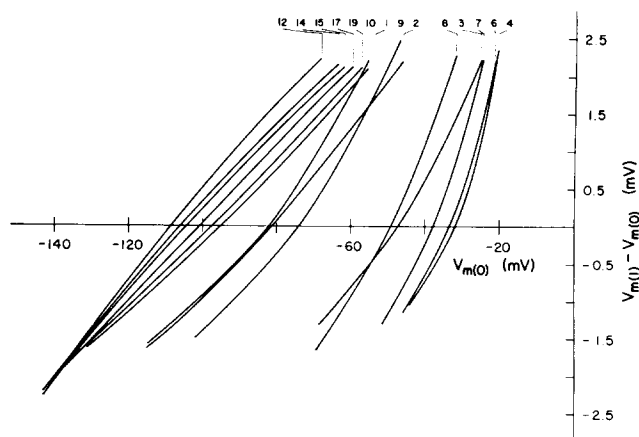


Fig. 4. Change of the current-voltage curve for the *Neurospora* plasma membrane, during the "action potential". Averaged data from 8 of the 12 "action potentials" in Experiment 4. Membrane current in the end cell is proportional to $V_{m(1)} - V_{m(0)}$, measured at the peak of each pulse; for a crosswall (pore) resistance of $2 \text{ M}\Omega$, 1 mV corresponds to 0.5 nA . Curves drawn by eye through 3 points: hyperpolarizing maximum, 0 current, and depolarizing maximum. Several numbered curves omitted for clarity. Curves 1–4 are from the phase of rapid depolarization; curves 6 and 7, during the plateau; curves 8–10, during the rapid repolarization; and curves 12–19, during the slow depolarization.

verted to current density with the factor $1/(2 \cdot 10^6 \cdot 58 \cdot 20\pi \cdot 10^{-8}) = 13.7 \mu\text{A} \cdot \text{cm}^{-2} \cdot \text{mV}^{-1}$. Current-voltage curves for the *Neurospora* membrane can be estimated, therefore, by plotting the values of $(\Delta V_{m(1)} - \Delta V_{m(0)})$ measured in Fig. 2 against $V_{m(0)}$. This method is similar to one introduced by Adrian and Freygang [20] for voltage clamp experiments on skeletal muscle. When such a plot was made for pulse-wise average values over all eight "action potentials" tested with current pulses, the curves of Fig. 4 were generated. (The pulses themselves were too brief (0.5 s) to trigger the "action potentials".) The numbers at the top of Fig. 4 are index numbers for the successive pulses, beginning at the onset of rapid depolarization. Each curve was drawn by eye through 3 points: the intercept, the hyperpolarizing (downward) maximum, and the depolarizing (upward) maximum for each pulse pair.

Fig. 4 makes clear that the membrane I-V curve of *Neurospora* becomes increasingly non-linear during the APL. At the start of slow depolarization (pulse 12) the I vs. V curve was somewhat convex upward, the slope conductance diminishing with depolarization. As depolarization proceeded, the non-linearity at first decreased, until, at pulse 17, the I vs. V curve was essentially linear. During the rapid rise of the "action potential" (pulse $1 \rightarrow 4$), however, the curve became strongly concave upward, membrane conductance increasing with pulsed depolarization.

A plot of the slope conductance at the voltage axis $(di_m/dV)_{i_m=0}$ versus time is shown in Fig. 5, along with the average voltage curve for the same eight "action potentials". Evidently, slow depolarization is accompanied by a slight decrease of membrane conductance (0.1 unit in Fig. 5, corresponding to $100 \mu\Omega^{-1} \cdot \text{cm}^{-2}$ for a depolarization of 15 mV); and the main part of the "action potential" occurs with a large increase of conductance (1 unit in Fig. 5, corresponding to $1 \text{ m}\Omega^{-1} \cdot \text{cm}^{-2}$, for the maximal depolarization).

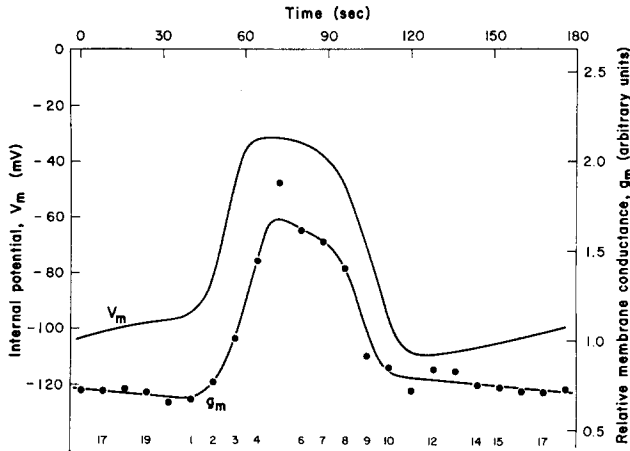


Fig. 5. Comparison of time courses of membrane potential and membrane conductance during the "action potential". Voltage curve is drawn through the intercept values in Fig. 4; each plotted point is the conductance read as the slope at the intercept on the like-numbered curve in Fig. 4. For a pore resistance (r_p) of $2 \text{ M}\Omega$, 1.0 unit on the conductance scale (right-hand ordinate) corresponds to $1 \text{ m}\Omega^{-1} \cdot \text{cm}^{-2}$.

The basic features from these conductance measurements were confirmed in Experiment 2, but in that case conductance increased from $150 \mu\Omega^{-1} \cdot \text{cm}^{-2}$, an 8-fold increase, compared with 2.5-fold (0.67 to 1.67 units) in Fig. 5. The quantitative difference may be accounted for by the lower resting conductance in Experiment 2: $150 \mu\Omega^{-1} \cdot \text{cm}^{-2}$, which compares with an estimated $670 \mu\Omega^{-1} \cdot \text{cm}^{-2}$ in Experiment 4 (estimate based on $r_p = 2 \text{ M}\Omega$). Then the same conductance, $1 \mu\Omega^{-1} \cdot \text{cm}^{-2}$, would be added at the peak of the "action potential" in each case.

Comments on condition velocity

Experiment 4 also provided data from which to investigate conduction velocity for the "action potentials", since in several records the normal current-passing electrode was used to record membrane potential, $260 \mu\text{m}$ distant from $V_{m(0)}$. The measured amplitude of the "action potential" was essentially identical at all three electrodes. An electrotonic space constant near $400 \mu\text{m}$ would be expected for the hypha in Experiment 4 (ref. 21), so that a non-conducted "action potential" localized near the fiber end should have been attenuated by about 40 % at a distance of $260 \mu\text{m}$, while one localized near (or to the right of) the current-passing electrode should have been attenuated about 20 % at the fiber end. It must be concluded, therefore, (a) that the "action potentials" were localized at a balanced position between the two extreme electrodes, which seems improbable, or (b) that "action potentials" were simultaneous over a large segment of hyphae, or (c) that they were conducted. The time resolution of the chart records is such that a conducted "action potential" could not have travelled slower than $100 \mu\text{m/s}$ from one electrode to the most distant electrode.

Voltage clamp experiments

Following the train of 12 "action potentials" seen in experiment 4 and described in Figs. 2, 4 and 5, spontaneous activity persisted for several more minutes,

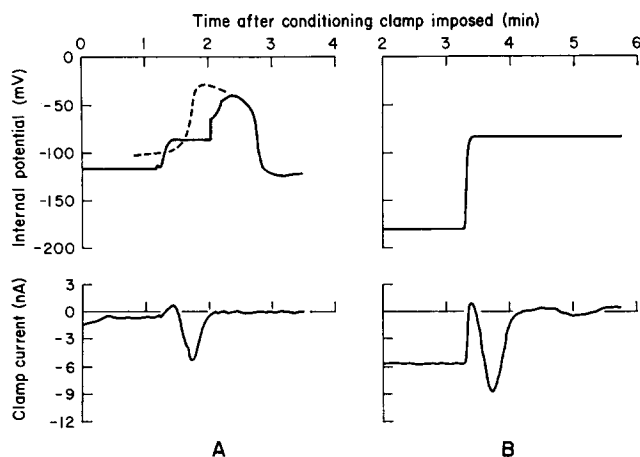


Fig. 6. "Action currents" in *Neurospora* (lower curves), measured during voltage clamping (upper curves). Experiment 4, voltage record $V_{m(1)}$. (A) 75-s prepulse at -117 mV before clamp potential was shifted through the action potential "threshold". Clamp at -86 mV held for 40 s, then switched off. Dashed curve in the upper half is a prior action potential superimposed on the residual action potential following release of the clamp. Peak current (lower trace) corresponds approximately to the steepest slope of the action potential. (B) 200-s prepulse at -180 mV before clamp potential was shifted through the threshold. Current in B is 55 % larger than in A.

and two tests were made in which $V_{m(1)}$ was clamped while the resultant current was measured. The voltage electrode in the 0th cell had been plugged off [22, 23] when these measurements were made, so the results are qualitative, but nevertheless interesting. They are shown in Fig. 6. In the first test (Fig. 6A) the membrane was hyperpolarized to -117 mV for 75 s, then changed to -86 mV for 40 s (upper record). During the 40-s interval, an inward current developed (lower record, Fig. 6A) which peaked at 5.4 nA after about 20 s. When the clamp was released, the membrane potential jumped to -64 mV and then drifted to -40 mV over a period of 18 s. Thereafter it executed a normal time-course for action potential-like repolarization. The repolarizing wave could be superimposed exactly on the preceding full "action potential" (dashed curve), so that the current peak can be seen to have been nearly simultaneous with the time of steepest rise of the action potential. In the second test (Fig. 6B), the initial clamp hyperpolarization went to -180 mV for 200 s, before the clamp was moved to -84 mV. The consequent inward current through the membrane executed the same time course as in the previous test, but was 55 % larger (8.4 nA). Unfortunately, since the clamp was non-uniform, and the current records give total current only, we cannot now assign a mechanistic interpretation to the results from the voltage-clamp experiment.

DISCUSSION

Thus far, the action potential-like behavior of *Neurospora* has been strictly a spontaneous event, a situation which severely limits the experiments that can be conducted; however, identification of the same phenomenon on four separate occasions does seem to justify a systematic search for permissive conditions. We have tried

several unsuccessful maneuvers to elicit the action potential-like behavior, including depolarization with pulses or steps of current, depolarization with pulses and steps of KCl or NaCl and treatment with a variety of inhibitors and ionophores.

Perhaps the most striking characteristic of the action potential-like behavior (other than its sporadicity) is its long duration, about 1 min excluding the initial slow depolarization. That is comparable to the duration of action potentials in the alga *Acetabularia* [24, 25], but is an order of magnitude longer than those of most other algae [26, 27] and higher plants [3, 4, 7–9] and is 5 orders of magnitude longer than the very fast action potential seen in nerve preparations [28]. The similarity between *Neurospora* action potential-like behavior and action potentials of certain cardiac muscle fibers [17, 18] extends beyond simply the general wave-form of membrane potential, and includes the conductance decrease associated with the phase of slow depolarization (pacemaker in heart muscle). However, the plateau of the action potential-like behavior differs from the plateau of Purkinje-fiber action potentials in being a high-conductance state. In this respect, it recalls the long-duration action potentials of fluoride-perfused squid giant axons [19].

There are two classes of mechanism which might explain this action potential-like behavior in *Neurospora*. The first was originally proposed by Van der Pol to describe the cardiac action potential [29–31] and has recently been partly revived by Gradmann to account for the action potential of *Acetabularia* [25]. It allows the fundamental current-voltage (I - V) relationship for the membrane to be fixed in shape, but non-linear: it could be either an N -shaped curve or a simple inverse sigmoid curve, the latter having already been reported for *Neurospora* [32, 33]. The “action potential”, then, would comprise the time-course of the voltage intercept as the membrane I - V curve is displaced downward along the current axis. Since the major fraction of the normal resting membrane potential in *Neurospora* results from electrogenic H^+ pumping [11, 13, 21], a diminution of the pump current could well serve to displace the membrane current-voltage curve downward along the current axis. Thus, the short current-voltage curves drawn in Fig. 4 could be seen roughly as segments of a complete curve having an inverse sigmoid shape. The high-conductance state existing during the peak and plateau of the “action potential” would result simply from the steepness of the I - V curve at the potential sustained by the minimum pump current. The time-course of the “action potential” would reflect both the shape of the I - V curve and the intrinsic time course of the pump current.

The second class of possible mechanism for the “action potential” in *Neurospora* is that now generally understood to account for the action potentials in classical excitable tissues: a change in the selectivity of the membrane which causes the membrane diffusion potential to shift (usually) in a depolarizing direction. This kind of action potential is associated with an inward (usually) ionic current carried by Na^+ in nerve and muscle [16, 28] and by Cl^- in the Characean algae [26, 34]. (An inward current of Na^+ , K^+ or Mg^{2+} can be ruled out as contributing to the “action potential” in *Neurospora*, since the equilibrium diffusion potentials for these ions lie substantially negative to the measured peaks of the “action potentials” (see Table III). The cations Ca^{2+} and H^+ cannot be eliminated in this fashion, nor can any of the anions. Of all inorganic ions present, H^+ and Cl^- seem most likely to carry inward current during the “action potential”; H^+ because it is known to be involved in a variety of other transport processes in *Neurospora* [11, 35, 39] and Cl^- by analogy

TABLE III

ESTIMATED IONIC DIFFUSION POTENTIALS ACROSS THE PLASMA MEMBRANE OF *NEUROSPORA*

Ions	Equilibrium diffusion potentials (mV)				Intracellular conc. (mM)	Refs.
	Expt. 1	Expt. 2	Expt. 3	Expt. 4		
K ⁺	-40	-50	-50	-73	180	36
Na ⁺	+15	—	—	—	14	36
H ⁺ (pH)	+41	+41	+41	+41	6.5	35
Ca ²⁺	—	++	++	++	μ M	—
Mg ²⁺	—	—	—	-44	16	37
Cl ⁻	-11	< +75	< +75	< +65	\geq 40	35
Phosphate*	++	-25/+7	++	-2/+18	10	38

* Total phosphate. At pH 5.8 phosphate is approximately 95 % in the H₂PO₄ form; and at pH 6.5, 80 %. Extracellular ion concentrations are given in Table I. — or ++ means large negative or large positive. — means slightly negative.

with Characean algae, the only group of non-animal cells which has been carefully studied.) The high-conductance state at the peak and plateau of the "action potential" would reflect the increase of membrane permeability that generates the "action potential", and the time-course of the "action potential" would reflect the intrinsic time course of the permeability change. The conductance decrease observed during slow depolarization might, as in Purkinje fibers [17], arise from a permeability decrease, but the ionic species involved is not clear; it cannot be K⁺, since the voltage range occupied by slow depolarization is in all instances negative to the equilibrium diffusion potential for K⁺.

At present there is no compelling evidence which would confirm or rule out either of these two possible mechanisms. Two qualitative arguments do seem to militate against the Van der Pol model: (a) the fact that none of the *I-V* curves presently available for the *Neurospora* membrane is sufficiently bent to yield the wave-form shown in Fig. 5 for voltage, when combined with a simple (e.g. sinusoidal or double-exponential) time-curve of pump current and (b) hysteresis, the fact that membrane conductance can be quite different at a given membrane potential, depending on whether the "action potential" is rising or falling (compare, for example, curve 3 and 8 in Fig. 4). These arguments notwithstanding, the Van der Pol model is still attractive, because it would unify the "action potentials" with the other, metabolically derived, oscillatory phenomena seen in *Neurospora* (Fig. 1), placing primacy on activity of the major electrogenic ion pump in the membrane. Clearly, however, demonstration of a mechanism for "action potentials" in *Neurospora* awaits discovery of a systematic method to elicit them.

ACKNOWLEDGEMENTS

These experiments were supported by Research Grant GM-15858 from the National Institute of General Medical Sciences, by Postdoctoral Fellowship F2-AM-16807 (to WSL) from the National Institute of Arthritis and Metabolic Diseases, and by Grants Gr 409/2 and Gr 409/5 (to DG) from the Deutsche Forschungsgemein-

schaft. The authors are indebted to Drs. U.-P. Hansen and R. W. Tsien for many useful comments on the manuscript.

REFERENCES

- 1 Finkelstein, A. (1964) *J. Gen. Physiol.* 47, 545-565
- 2 Eckert, R. (1972) *Science* 176, 473-481
- 3 Sibaoka, T. (1962) *Science* 137, 226
- 4 Sibaoka, T. (1973) *Bot. Mag. Tokyo* 86, 51-61
- 5 Stuhlman, O. and Darden, E. B. (1950) *Science* 111, 491-492
- 6 Williams, S. E. and Pickard, B. G. (1972) *Planta* 103, 222-240
- 7 Sinyukhin, A. M. and Gorchakov, V. V. (1966) *Sov. Plant Physiol.* 13, 727-733
- 8 Sinyukhin, A. M. and Gorchakov, V. V. (1966) *Biophysics* 11, 840-846
- 9 Pickard, B. G. (1972) *Planta* 102, 91-114
- 10 Vogel, H. J. (1956) *Microb. Gen. Bull.* 13, 42
- 11 Slayman, C. L., Long, W. S. and Lu, C.Y.-H. (1973) *J. Membrane Biol.* 14, 305-338
- 12 Huxley, A. F. (1961) *J. Physiol.* 157, 5-7P
- 13 Slayman, C. L. (1965) *J. Gen. Physiol.* 49, 69-92
- 14 Lambowitz, A. M. and Slayman, C. W. (1971) *J. Bacteriol.* 108, 1087-1096
- 15 Gradmann, D. and Slayman, C. L. (1975) *J. Membrane Biol.* 23, 181-212
- 16 Noble, D. (1966) *Physiol. Rev.* 46, 1-50
- 17 Noble, D. and Tsien, R. W. (1968) *J. Physiol.* 195, 185-214
- 18 West, T. C. (1972) in *Electric Phenomena in the Heart* (DeMello, W. C., ed.), pp. 191-217, Academic Press, New York
- 19 Chandler, W. K. and Meves, H. (1970) *J. Physiol.* 211, 707-728
- 20 Adrian, R. H. and Freygang, W. H. (1962) *J. Physiol.* 163, 61-103
- 21 Slayman, C. L. (1965) *J. Gen. Physiol.* 49, 93-116
- 22 Umrath, K. (1932) *Protoplasma* 16, 173-188
- 23 Walker, N. A. (1955) *Aust. J. Biol. Sci.* 8, 477-489
- 24 Gradmann, D. and Bentrup, F. W. (1970) *Naturwiss.* 57, 46-47
- 25 Gradmann, D. (1976) *J. Membrane Biol.*, submitted for publication
- 26 Kishimoto, U. (1965) *J. Cell. Comp. Physiol.* 66, 43-54
- 27 Findlay, G. P. and Hope, A. B. (1964) *Aust. J. Biol. Sci.* 17, 400-411
- 28 Hodgkin, A. L. and Huxley, A. F. (1952) *J. Physiol.* 116, 497-506
- 29 Van der Pol, B. (1926) *Phil. Mag.* 2, 978-992
- 30 Van der Pol, B. and Van der Mark, J. (1928) *Phil. Mag. Suppl.* 6, 763-775
- 31 Jack, J. J. B., Noble, D. and Tsien, R. W. (1975) *Electric Current Flow in Excitable Cells*, pp. 323-330, Clarendon Press, Oxford
- 32 Slayman, C. L. and Gradmann, D. (1975) *Biophys. J.* 15, 968-971
- 33 Slayman, C. L. and Gradmann, D. (1973) *Abstr. Annu. Meet. Biophys. Soc.* Item TAM-J10
- 34 Findlay, G. P. (1970) *Aust. J. Biol. Sci.* 23, 1033-1045
- 35 Slayman, C. L. and Slayman, C. W. (1968) *J. Gen. Physiol.* 52, 424-443
- 36 Slayman, C. W. and Tatum, E. L. (1964) *Biochim. Biophys. Acta* 88, 578-592
- 37 Viotti, A., Bagni, N., Sturani, E. and Alberghina, F. A. M. (1971) *Biochim. Biophys. Acta* 244, 329-337
- 38 Harold, F. M. (1962) *J. Bacteriol.* 83, 1047-1057
- 39 Slayman, C. L. and Slayman, C. W. (1974) *Proc. Natl. Acad. Sci. U.S.* 71, 1935-1939